An Adaptive Triggering Method for Capturing Peak Samples in a Thin Phytoplankton Layer by an Autonomous Underwater Vehicle

Yanwu Zhang, *Senior Member, IEEE*, Robert S. McEwen, *Member, IEEE*, John P. Ryan, and James G. Bellingham

***Abstract*—Thin layers of phytoplankton have important impacts on coastal ocean ecology. The high spatial and temporal variability of such layers makes autonomous underwater vehicles (AUVs) ideal for their study. We have used an AUV for obtaining repeated high-resolution surveys of thin layers in Monterey Bay, California. The AUV is equipped with ten "gulpers" that can capture water samples when some feature is detected. In this paper, we present an adaptive triggering method for an AUV to capture water samples at fluorescence peaks in a thin layer. The presented method is tested by AUV data from the 2005 Layered Organization in the Coastal Ocean (LOCO) field program in Monterey Bay. Field tests will be conducted in upcoming AUV cruises.**

***Index Terms*—Autonomous underwater vehicle (AUV), peak detection, water sample acquisition, thin phytoplankton layer.**

I. Introduction

Thin layers of phytoplankton are often observed in the coastal ocean [1]–[4]. They have important impacts on the patterns of primary productivity, the survival and growth of zooplankton and fish larvae, the development of harmful algal blooms (HABs), and other aspects of coastal ocean ecology [3]. The thin layers have a thickness ranging from < 1 m to a few meters, and can horizontally extend for kilometers [1]–[4]. For studying the thin layers, high-resolution sampling in the vertical direction is required.

At the Monterey Bay Aquarium Research Institute (MBARI), we run a Dorado AUV [5], [6] to conduct surveys of thin phytoplankton layers. The vehicle has a length of 4.2 m and a diameter of 0.53 m at the midsection. Its sensor suite includes SeaBird SBE25 temperature and conductivity sensors, a Paroscientific 8CB4000-I pressure sensor, and a HOBI Labs HydroScat-2 sensor that measures chlorophyll fluorescence at the 676-nm wavelength and backscatter at the 470-nm and 676-nm wavelengths. While in situ measurements are essential for an AUV survey, many important chemical and biological properties of seawater can only be measured in the laboratory, which calls for collecting water samples and returning them to shore. AUV-borne water samplers are particularly needed for the studies of plankton and larval ecology, primary production, and HABs [7]. MBARI engineers designed and installed ten 2-liter "gulpers" [8] on an Dorado AUV, which can capture water samples when some feature is detected.

All authors are with the Monterey Bay Aquarium Research Institute, 7700 Sandholdt Road, Moss Landing, CA 95039. Email of the corresponding author Yanwu Zhang: yzhang@mbari.org

0-933957-38-1 ©2009 MTS

Within a thin layer, a high biomass concentration leads to a high level of chlorophyll fluorescence [4]. Therefore, for investigating the peak biomass, it is a critical task to have the gulpers capture water samples at fluorescence peaks. As a first step, the second and third authors devised and field-tested a method of triggering a gulper capture when the AUV's fluorescence measurement exceeds a pre-set threshold. For robustness, they added a requirement that a number of consecutive measurements should all exceed the threshold before a gulper can be triggered. The approach was successful in triggering the gulpers for capturing water samples above some fluorescence threshold, but how to capture water samples at fluorescence peaks remains a challenge.

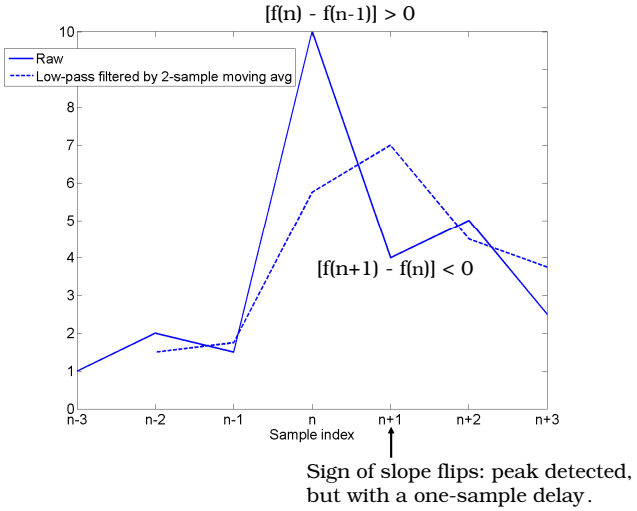

Fig. 1. If using slope tracking for real-time peak detection, the detection would come late.

Real-time peak detection is a difficult problem. The basic approach of gradient (i.e., slope) tracking — declaring a peak when the sign of the slope flips from positive to negative [9], works well in postprocessing, but not in real time: when it is found that the gradient has just turned negative, the peak has already passed. As a result, peak detection would come late. To prevent false peak detections caused by noise spikes or minor bumps, low-pass filtering is commonly required, which adds an additional delay in peak detection.

An example of peak detection is illustrated in Figure 1. On the raw measurement (the solid curve), the peak lies at time index n, but the flipping of the slope's sign can only be detected at $n+1$. Hence the peak detection on the solid curve comes late at $n+1$. Note that the raw measurement has two minor peaks at $n-2$ and $n+2$. To remove those two minor peaks, we low-pass filter the raw measurement by a 2-sample moving-average window, resulting in the dashed curve. This low-pass filtering carries a delay of one sample, hence "moving" the peak from n to $n+1$. Consequently, peak detection by gradient tracking on the dashed curve comes at $n+2$. Thus the total delay in peak detection is now two samples. In practice, more intense low-pass filtering is often required to suppress stronger noise, which means an even longer delay. For instance, a 7-sample moving-average window will cause a delay of $\frac{7-1}{2} = 3$ samples. Then the total delay in peak detection will be $3+1 = 4$ samples. The sampling interval of the HydroScat-2 fluorescence and backscatter sensor is 0.25 second. So a 4-sample delay means a delay of 1 second. If an AUV carries a HydroScat-2 sensor and crosses a thin layer of a 0.5-m thickness at a vertical speed of 0.5 m/s, a 1-second delay means that the AUV will miss the layer.

Another type of approach, under the premise that the signal shape is known *a priori*, employs the technique of matched filtering [10] for peak detection [11], [12]. However, not only is the computation more complicated, but also the variability of oceanographic signals often makes it infeasible to assume a signal shape *a priori*.

To enable an AUV to capture peaks without delay, we have devised a novel method that takes advantage of the vehicle's sawtooth (i.e., "yo-yo") trajectory. The method will be described in Section II. Tests by AUV data from a previous field experiment will be presented in Section III. Real-time field tests are to be conducted in upcoming AUV cruises, as will be proposed in Section IV.

II. A Novel Method for Real-Time Peak Detection and Triggering for an AUV Gulper

A. Overview

In a thin phytoplankton layer, the chlorophyll fluorescence and backscatter levels are at least several times higher than the background levels [3], [4]. When an AUV traverses the layer, it can detect a fluorescence peak. As discussed in Section I, peak detection cannot escape a delay in a single crossing of the layer. However, in an ascent-descent cycle (i.e., a "yo-yo cycle"), the AUV makes two crossings of the layer, as illustrated in Figure 2. The basic idea of our method is to have the AUV detect the fluorescence peak and save the peak height on the first crossing (although the detection comes with a delay, the peak height is properly saved), and capture the peak with no delay on the second crossing, assuming the peak value persists over the short distance.

First, a running-average (from the start time to present) of the raw fluorescence measurement is calculated to provide the background level:

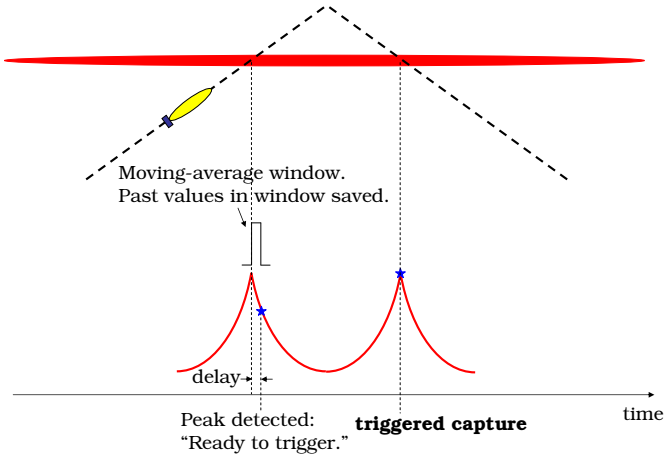

Fig. 2. On its yo-yo trajectory through a thin phytoplankton layer, an AUV detects the fluorescence peak on the first crossing, with a delay. It captures the peak on the second crossing with no delay.

$$FL_{background}(n) = \frac{1}{n+1}\sum_{i=0}^{n} FL(i) = \frac{FL_{background}(n-1)*n + FL(n)}{n+1} \quad (1)$$

where i is the time index; n is the index of the current time; $FL(i)$ is the raw fluorescence measurement.

Likewise, running-averages of the raw backscatter measurements are calculated to provide the background levels:

$$BB_{470nm\_background}(n) = \frac{1}{n+1}\sum_{i=0}^{n} BB_{470nm}(i) = \frac{BB_{470nm\_background}(n-1)*n + BB_{470nm}(n)}{n+1} \quad (2)$$

$$BB_{676nm\_background}(n) = \frac{1}{n+1}\sum_{i=0}^{n} BB_{676nm}(i) = \frac{BB_{676nm\_background}(n-1)*n + BB_{676nm}(n)}{n+1} \quad (3)$$

where $BB_{470nm}(i)$ and $BB_{676nm}(i)$ are the raw backscatter measurements at the 470-nm and 676-nm wavelengths, respectively.

To reduce spurious peaks due to noise, the raw measurements are low-pass filtered by an M-sample moving-average window:

$$FL_{lp}(n) = \frac{1}{M}\sum_{i=0}^{M-1} FL(n-i) \quad (4)$$

$$BB_{470nm\_lp}(n) = \frac{1}{M}\sum_{i=0}^{M-1} BB_{470nm}(n-i) \quad (5)$$

$$BB_{676nm\_lp}(n) = \frac{1}{M}\sum_{i=0}^{M-1} BB_{676nm}(n-i) \quad (6)$$

Two main criteria for a thin phytoplankton layer are: (1) The peak fluorescence value exceeds twice the background level. (2) There is a corresponding peak in backscatter [4]. To avoid noise-induced peaks, we use low-passed signals to check against the criteria. A detected peak of fluorescence qualifies as a "real peak" only when both criteria are met:

$$\begin{aligned} &\text{If } \frac{FL_{lp}(n)}{FL_{background}(n)} \geq \alpha_{fl} \text{ AND} \\ &\quad \Big[\frac{BB_{470nm\_lp}(n)}{BB_{470nm\_background}(n)} \geq \alpha_{bb} \text{ OR} \\ &\qquad \frac{BB_{676nm\_lp}(n)}{BB_{676nm\_background}(n)} \geq \alpha_{bb}\Big], \\ &\text{a "real peak" is detected: } FL\_PEAK(i) = FL_{lp}(n) \end{aligned} \quad (7)$$

where i is the peak index; $\alpha_{fl} > 1$ and $\alpha_{bb} > 1$ are two ratio thresholds. According to the first criterion in the above, we set α_{fl} to 2. As for α_{bb}, we set it to 2 in the tests in Section III. Its optimal setting requires further statistical analysis of the data. The thresholds for a "real peak" are thus adaptively adjusted in real time.

The mechanism of our peak-detection and triggering method is depicted in Figure 2. On the vehicle's first crossing on the ascent leg, the peak detection comes with a delay. However, we let the vehicle save past raw measurements of fluorescence within the moving-average window (i.e., the low-pass filter). This way, although the vehicle has just missed the peak (due to the delay of the detection) on the first crossing, it has saved the true peak height.

Since the AUV is equipped with only ten gulpers, their triggerings should only occur on high fluorescence peaks. For this purpose, the running-average of the detected fluorescence peaks is taken as the peaks' baseline:

$$\begin{aligned} FL\_PEAK_{baseline}(k) &= \frac{1}{k+1}\sum_{i=0}^{k} FL\_PEAK(i) \\ &= \frac{FL\_PEAK_{baseline}(k-1) * k + FL\_PEAK(k)}{k+1} \end{aligned} \quad (8)$$

where i is the peak index; k is the number of detected peaks up to present; $FL\_PEAK(i)$ is the value of the detected peak. Only those peaks that are above $FL\_PEAK_{baseline}(k)$ qualify as "high peaks":

$$FL_{lp}(n) > FL\_PEAK_{baseline}(k) \quad (9)$$

Thus the threshold for a "high peak" is also adaptively adjusted in real time.

Presuming the fluorescence peak detected on the first crossing exceeds the threshold $FL\_PEAK_{baseline}$, then at the second crossing on the descent leg (in Figure 2), the vehicle is likely to encounter the peak again due to the thin layer's horizontal extent. As the two adjacent crossings are only separated by a short distance, the two peak measurements should have very similar heights. On the second crossing, as soon as the raw fluorescence measurement reaches the saved peak height (plus meeting additional timing and depth conditions that will be given in Subsection II-D), an AUV gulper is triggered. As a thin layer's intensity varies over distance, the peak heights at the first and second crossings may have a small difference. If the second peak is lower than the first (i.e., the saved peak height), there will be no triggering. This actually serves our objective of triggering gulpers only on high peaks. Conversely, if the second peak is slightly higher than the first, the gulper will be triggered slightly before the second peak arrives. Since the water sample takes $1 \sim 2$ seconds to fill the gulper, a slightly early triggering means that the peak will arrive in the middle of the short gulping process.

The key components of the peak detection and triggering algorithm are elaborated upon in the following subsections.

B. Peak Detection by Slope Tracking

For fluorescence peak detection on the first crossing, we employ the basic approach of slope tracking. We define a state variable [13] S_{FL}, and two other variables FL_{max} and FL_{min} for storing the maximum and minimum fluorescence values. The definitions of the states are as follows,

$$\begin{aligned} &\text{If } FL_{lp}(n) > FL_{max}, \\ &\text{set } S_{FL}(n) \text{ to 1, and update } FL_{max} \text{ by } FL_{lp}(n). \\ &\text{If } FL_{lp}(n) < FL_{min}, \\ &\text{set } S_{FL}(n) \text{ to 0, and update } FL_{min} \text{ by } FL_{lp}(n). \end{aligned} \quad (10)$$

A fluorescence peak is detected when S_{FL} changes from 1 to 0 (i.e., the slope changes from being positive to being negative). To prevent false state changes due to noise, we set two low-value thresholds δ_{FL_rise} and δ_{FL_drop} (both are positive numbers). Only a rise/drop that exceeds the corresponding threshold is considered significant enough to qualify as a non-trivial rise/drop. State changes occur as follows,

$$\begin{aligned} &\text{If } S_{FL}(n-1) = 1 \text{ AND} \\ &\quad \Big[\big[FL_{lp}(n) - FL_{max} < -\delta_{FL\_drop}\big] \text{ OR} \\ &\qquad \big[FL_{lp}(n) \text{ has dropped twice in a row}\big]\Big], \\ &\text{set } S_{FL}(n) \text{ to 0. A peak is detected.} \end{aligned}$$

$$\begin{aligned} &\text{If } S_{FL}(n-1) = 0 \text{ AND } FL_{lp}(n) - FL_{min} > \delta_{FL\_rise}, \\ &\text{set } S_{FL}(n) \text{ to 1.} \end{aligned} \quad (11)$$

C. Timing of the First-Peak Detection and the Subsequent Triggering: on an Ascent Leg or a Descent Leg?

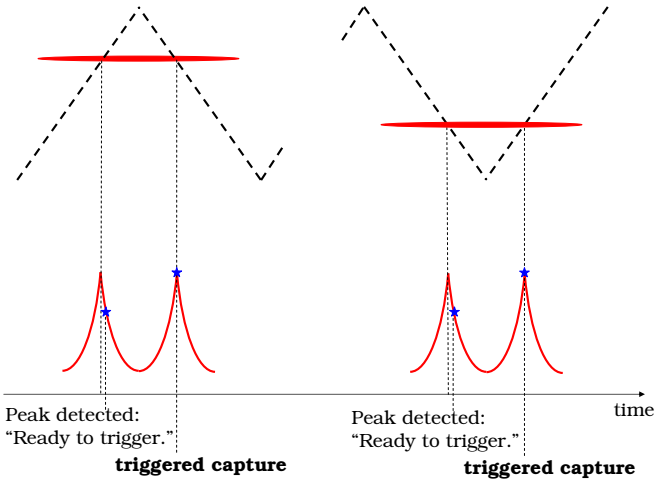

Fig. 3. The AUV determines the timing of the first-peak detection and the subsequent triggering based on whether the thin layer lies in the upper or lower half of the AUV's yo-yo profile.

The threshold for triggering at the second crossing is set by the peak height saved at the first crossing. To ensure that the two peaks have about the same height, we need to keep the separation between the pair of crossings small. If the thin layer lies in the upper half of the yo-yo profile, the first-peak detection should occur on the ascent leg and the subsequent triggering should occur on the descent leg (as shown in the left panel in Figure 3). Conversely, if the thin layer lies in the lower half of the yo-yo profile, the first-peak detection should occur on the descent leg and the subsequent triggering should occur on the ascent leg (as shown in the right panel in Figure 3).

Using the same algorithm as presented in Subsection II-B, the AUV tracks the state of its own depth by a variable S_{DEP} ($S_{DEP} = 1$: descending; $S_{DEP} = 0$: ascending), and tracks the maximum and minimum depths by variables DEP_{max} and DEP_{min}. The real-time mid-depth of the vehicle is $DEP_{mid} = \frac{DEP_{max}+DEP_{min}}{2}$.

When a fluorescence peak is detected on the first crossing, the corresponding depth $DEP(n)$ is compared with DEP_{mid}. Only if $S_{DEP} = 1$ (i.e., the AUV is descending) plus $DEP(n) > DEP_{mid}$ (i.e., the thin layer lies in the lower half of the yo-yo profile), or $S_{DEP} = 0$ (i.e., the AUV is ascending) plus $DEP(n) < DEP_{mid}$ (i.e., the thin layer lies in the upper half of the yo-yo profile), does the peak qualify as a "pre-trigger peak" (for a subsequent triggering on the second crossing).

D. Additional Conditions for Triggering a Gulper

For triggering a gulper on the second crossing, besides the condition of reaching the fluorescence peak value (saved on the first crossing), we add two additional conditions:

1) Since the AUV carries only ten gulpers, we set a minimum time interval T_{min} between triggerings to prevent using up gulpers over a short distance. A triggering is allowed only if the elapsed time since the last triggering exceeds T_{min}.
2) To prevent gulping air bubbles, a triggering is allowed only if the vehicle's depth exceeds a threshold DEP_{thresh}.

III. Tests by AUV Field Data

An MBARI Dorado AUV was deployed in the 2005 Layered Organization in the Coastal Ocean (LOCO) field program in Monterey Bay, California [4]. The vehicle ran in a yo-yo trajectory at a pitch angle of about 17° and a forward speed of about 1.75 m/s. We use the LOCO AUV data to test the presented method. The length of the low-pass filtering moving-average window is set to 8.

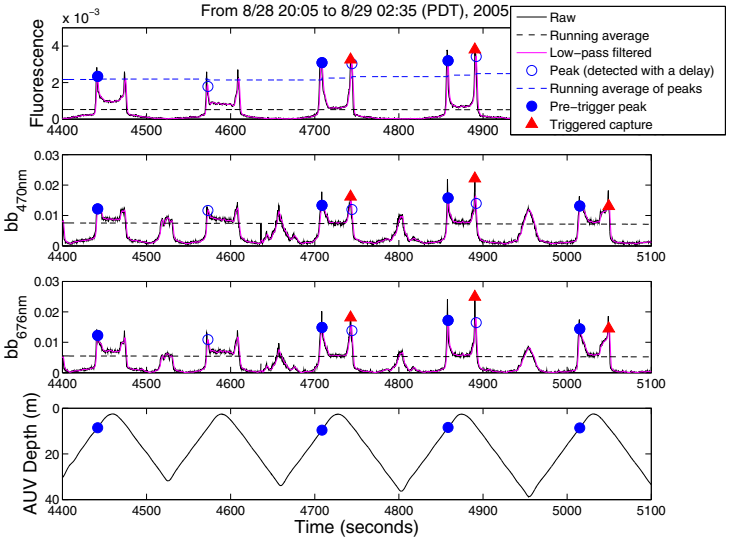

Fig. 4. Peak detection and triggering using Dorado AUV data in Mission 2005.241.02. In this section, the thin layer lies in the upper half of the yo-yo profile. The x-axis is the elapsed time since the start of the mission.

Figure 4 displays peak detection and triggering in a section of a mission on 28-29 August 2005. First, let us look at the AUV's two crossings near 4900 s. On the first crossing, a fluorescence peak is detected (marked by the blue solid circle). It passes three successive tests to qualify as a "pre-trigger peak":

1) Since both criteria in Equation (7)) are met, the peak qualifies as a "real peak".
2) Furthermore, since the peak height exceeds the peaks' baseline (the blue dashed line), the peak qualifies as a "high peak".
3) When the peak is detected, $S_{DEP} = 0$ (i.e., the AUV is ascending) and $DEP(n) < DEP_{mid}$ (i.e., the thin layer lies in the upper half of the yo-yo profile). Hence the peak qualifies as a "pre-trigger peak".

On the second crossing, when the fluorescence measurement reaches the peak height saved on the first crossing, a gulper is

triggered (marked by the red solid triangle). This high peak is successfully captured. Similarly, a high peak is captured near 4700 s. The distance between two adjacent crossings is about 50 m. Note that the thresholds for a "real peak" and a "high peak" are adaptively adjusted by new measurements in real time. In order to test the algorithm's ability to capture all high peaks, we do not set the minimum time interval T_{min} between triggerings, nor the minimum depth DEP_{thresh} for triggering. In field experiments, we will set those two parameters.

Near 4450 s, on the first crossing, a fluorescence peak is detected and it qualifies as a "pre-trigger peak" (the blue solid circle). However, on the second crossing, the fluorescence measurement does not reach the peak height saved on the first crossing. Consequently, no triggering occurs.

Near 4600 s, on the first crossing, a fluorescence peak is detected (the blue open circle), However, since the peak height is below the peaks' baseline (the blue dashed line), the peak does not qualify as a "high peak". Hence it is not a "pre-trigger peak", and no triggering occurs on the second crossing.

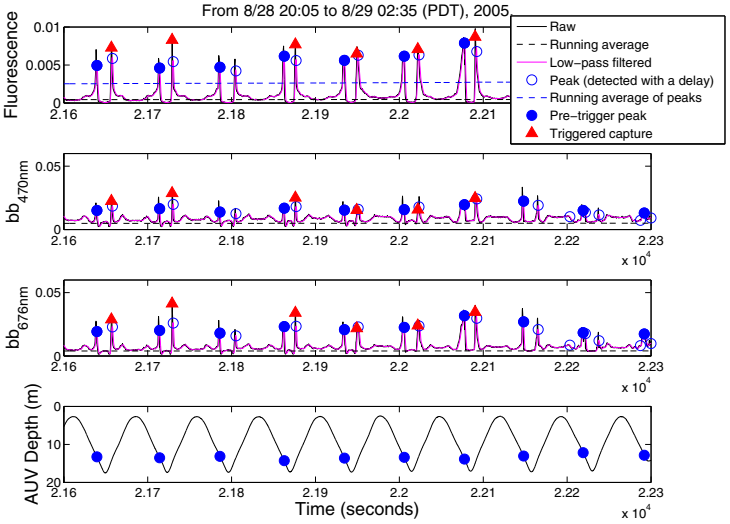

Fig. 5. Peak detection and triggering using Dorado AUV data in Mission 2005.241.02. In this section, the thin layer lies in the lower half of the yo-yo profile.

Figure 5 displays peak detection and triggering in another section of the mission. In this section, the thin layer lies in the lower half of the yo-yo profile. The distance between two adjacent crossings is about 20 m.

IV. Future Work

The purpose of setting a minimum time interval T_{min} between triggerings is to prevent using up the gulpers over a short distance. If T_{min} is too small, the AUV may run out of gulpers too early, before more significant fluorescence signals show up. If T_{min} is too large, the AUV may miss significant fluorescence signals and end up with empty gulpers. Therefore, T_{min} should be adaptively adjusted instead of being set as a constant. Following the scheme in [14], T_{min} can be adjusted based on the number of triggerings so far and the signal strength. If the fluorescence signal is strong and the number of triggerings so far is low, T_{min} needs to be reduced to allow for more triggerings, expressed as follows,

$$\text{If } \Big[\big[\frac{FL_{lp}(n)}{FL\_PEAK_{baseline}(k)} > \beta\big] \text{ AND } \big[N_{gulpers\_triggered} < N_{gulpers\_total}\frac{T_{elapsed}}{T_{mission\_total}}\big]\Big], \quad (12)$$

reduce T_{min}.

where $N_{gulpers\_total}$ and $N_{gulpers\_triggered}$ are the total number of gulpers and the number of triggerings so far, respectively. $T_{mission\_total}$ and $T_{elapsed}$ are the total mission time and the elapsed time, respectively. $\beta > 1$ is a ratio threshold whose value is yet to be determined.

In upcoming AUV surveys of thin phytoplankton layers in Monterey Bay, we will apply the presented method for capturing peak-fluorescence water samples.

Acknowledgment

This work was supported by the David and Lucile Packard Foundation. The authors are thankful to Michael McCann for the help with accessing the archived Dorado AUV data.

References

[1] T. J. Cowles, R. A. Desiderio, and M.-E. Carr, "Small-scale planktonic structure: Persistence and trophic consequences," *Oceanography*, vol. 11, no. 1, pp. 4–9, 1998.

[2] M. A. McManus, R. M. Kudela, M. W. Silver, G. F. Steward, P. L. Donaghay, and J. M. Sullivan, "Cryptic blooms: Are thin layers the missing connection?" *Estuaries and Coasts: J CERF*, vol. 31, pp. 396–401, 2008.

[3] J. P. Ryan, M. A. McManus, J. D. Paduan, and F. P. Chavez, "Phytoplankton thin layers caused by shear in frontal zones of a coastal upwelling system," *Marine Ecology Progress Series*, vol. 354, pp. 21–34, 2008.

[4] J. P. Ryan, M. A. McManus, and J. M. Sullivan, "Interacting physical, chemical and biological forcing of phytoplankton thin-layer variability in Monterey Bay, California," *Continental Shelf Research*, accepted for publication, 2009.

[5] J. G. Bellingham, K. Streitlien, J. Overland, S. Rajan, P. Stein, J. Stannard, W. Kirkwood, and D. Yoerger, "An Arctic basin observational capability using AUVs," *Oceanography*, vol. 13, no. 2, pp. 64–71, 2000.

[6] D. R. Thompson, "AUV operations at MBARI," *Proc. MTS/IEEE Oceans'07*, pp. 1–6, October 2007, Vancouver, Canada.

[7] "Lowering the threshold for ocean access," *Monterey Bay Aquarium Research Institute Annual Report*, pp. 9–12, 2005.

[8] L. E. Bird, A. Sherman, and J. Ryan, "Development of an active, large volume, discrete seawater sampler for autonomous underwater vehicles," *Proc. MTS/IEEE Oceans'07*, pp. 1–5, October 2007, Vancouver, Canada.

[9] G. Vivó-Truyols, J. R. Torres-Lapasió, A. M. van Nederkassel, Y. V. Heyden, and D. L. Massart, "Automatic program for peak detection and deconvolution of multi-overlapped chromatographic signals. Part I: Peak detection," *Journal of Chromatography A*, vol. 1096, pp. 133–145, 2005.

[10] H. L. Van Trees, *Detection, Estimation, and Modulation Theory, Part I*. New York, NY: John Wiley and Sons, Inc., 1968.

[11] V. P. Andreev, T. Rejtar, H.-S. Chen, E. V. Moskovets, A. R. Ivanov, and B. L. Karger, "A universal denoising and peak picking algorithm for LC-MS based on matched filtration in the chromatographic time domain," *Analytical Chemistry*, vol. 75, pp. 6314–6326, 2003.

[12] P. Du, W. A. Kibbe, and S. M. Lin, "Improved peak detection in mass spectrum by incorporating continuous wavelet transform-based pattern matching," *Bioinformatics*, vol. 22, no. 17, pp. 2059–2065, 2006.

[13] V. T. Jordanov, D. L. Hall, and M. Kastner, "Digital peak detector with noise threshold," *Proc. IEEE Nuclear Science Symposium*, vol. 1, pp. 140–142, November 2002, Norfolk, VA.

[14] Y. Zhang, J. G. Bellingham, and J. W. Bales, "Event triggering for AUV missions in the Labrador Sea Experiment," MIT Sea Grant AUV Lab, Technical Report, November 1997.